High-pressure behavior of polyiodides confined into single-walled carbon nanotubes: A Raman study

L. Alvarez,[1] J.-L. Bantignies,[1] R. Le Parc,[1] R. Aznar,[1] J.-L. Sauvajol,[1] A. Merlen,[2] D. Machon,[3] and A. San Miguel[3]
[1]*LCVN, University Montpellier 2, UMR 5587, 34095 Montpellier Cedex 05, France*
[2]*IM2NP, Université du Sud Toulon-Var, UMR 6242, BP 20132, F-83957 La Garde Cedex, France*
[3]*Laboratoire PMCN, UMR 5586, Université Lyon 1, CNRS–Université de Lyon, Villeurbanne 69622, France*
(Received 22 July 2010; revised manuscript received 23 September 2010; published 4 November 2010)

The high-pressure behavior of polyiodides confined into the hollow core of single-walled carbon nanotubes organized into bundles has been studied by means of Raman spectroscopy. Several regimes of the structural properties are observed for the nanotubes and the polyiodides under pressure. Raman responses of both compounds exhibit correlations over the whole pressure range (0–17 GPa). Modifications, in particular, take place, respectively, between 1 and 2.3 GPa for polyiodides and between 7 and 9 GPa for nanotubes, depending on the experiment. Differences between one experiment to another are discussed in terms of nanotube filling homogeneity. These transitions can be presumably assigned to the tube ovalization pressure and to the tube collapse pressure. A nonreversibility of several polyiodide mode modifications is evidenced and interpreted in terms of a progressive linearization of the iodine polyanions and a reduction in the charged species on pressure release. Furthermore, the significant change in the mode intensities could be associated to an enhancement of lattice modes, suggesting the formation of a new structure inside the nanotube. Changes in the nanotube mode positions after pressure release point out a decrease in the charge transfer in the hybrid system consistent with the observed evolution of the charged species.

DOI: 10.1103/PhysRevB.82.205403 PACS number(s): 78.30.Na, 78.70.En

I. INTRODUCTION

Single-walled carbon nanotubes (SWCNTs) represent ideal nanoconfinement systems owing to their one-dimensional (1D) hollow core with diameter comprised between 0.7 and 2 nm.[1,2] The introduction of foreign species into these 1D nanocavities leads to novel and exciting effects both for the filling entities and the host carbon matrix.[2–4] The physical properties of the confined material can differ significantly from those of the bulk.[2] In fact, original quantum effects can arise from the low-dimensional confinement imposed by the nanotubes as well as by guest-host interactions. For instance, Guan *et al.*[5] suggest the formation of a really new iodine phase depending on the tube diameters and due the confinement effect. Furthermore, reducing the tube diameters could allow to synthesize a linear atomic wire of iodine, which would be one ultimate quantum object.[5]

Iodine is a typical *p*-type dopant very stable inside SWCNT.[5–8] It gives rise to charge-transfer complexes, leading to I_n^{-m} anions (polyiodides) and SWCNT cations. Very recently, it has been shown that a temperature treatment can allow the tuning of charge transfer on iodine intercalated nanotube.[8] Thus, controlling the thermodynamic conditions could allow modifying the nanotube transport properties by switching the charge transfer on the tube, opening a way of getting tunable electronic properties of air stable nanocompounds. However, little is known about the physical and especially structural properties of the inserted iodine species. The structural and electronic properties of the confined polyiodides into SWCNT (I@SWCNT) have been investigated by different experimental methods. Transmission electron microscopy (TEM) investigations report the formation of either helicoidal chains[5,6] or new crystalline structures depending on the tube diameter.[6] By contrast, Raman spectroscopy measurements suggest the presence of short polyiodide chains (I_3^- and I_5^-) in SWCNT (Refs. 9–13) in good agreement with typical iodine charge-transfer complexes in other organic systems.[14–19] Furthermore, extended x-ray-absorption fine structure (EXAFS) studies on I@SWCNT support the presence only of disordered I_5^- anion chains.[12] In summary, the precise structural and electronic properties of the polyiodides within SWCNT still remain under debate. In this context, the application of high pressure, which allows the continuous modification of host-guest interactions, constitutes a powerful tool not only for clarifying the ambient conditions of the guest species under nanoconfinement but also to explore new opportunities arising from the modifications caused by these modulated interactions.

Iodine molecule (I_2) and the Lewis base donors I^- and I_3^- can be regarded as the main building blocks of polyiodides.[16–18] Polyiodides do not exist as discrete entities but are always a combination of I_2 molecules and I^- and/or I_3^- anion chains.[14,18] They can be described by the following formula: $mI_2+nI^- \rightarrow I_{(2m+n)}^{n-}$ leading to several possible structures. For instance, I_3^- might be a three-body system (I-I-I, I_3^- entity) or an asymmetric anions consisting in I_2 molecule weakly interacting with I^- ion.[14–19] In the same way, an I_5^- anion can be described as an I_3^- entity associated to an I_2 molecule ($I_3^- \cdot I_2$) or as two I_2 molecules in interaction with an I^- ion ($2I_2 \cdot I^-$). In addition, polyiodides can display several shapes such as linear, V or L shaped. Table I reports the Raman mode frequencies for the main short I_n^{-m} chains reported in the literature.[14–19]

Under high-pressure halogens are known to follow several phase transformations including a change on the intrabond characteristics corresponding to a loss of molecular character which has been identified in bromine at 25 GPa.[20] The Raman features associated to the 25 GPa phase transi-

 ©2010 The American Physical Society

TABLE I. Raman mode frequencies for main short polyiodides reported from literature. s=strong, m=medium, and w=weak.

Iodine species	Raman frequencies (cm^{-1})	References
I_2	174 s	14–18
Symmetric I_3^- $(I\text{-}I\text{-}I)^-$	110 s	14–19
Asymmetric I_3^- $(I_2 \cdot I^-)$	167 s, 143 w, 114 w	14–17
I_5^- linear $(I_2 \cdot I^- \cdot I_2)$	160 s, 104 w	14–17
I_5^- V shaped $(I_2 \cdot I^- \cdot I_2)$	167 s, 131 m, 114 w	16
I_5^- L shape $(I_3^- \cdot I_2)$	164 s, 135 m, 106 w	17

tion observed in bromine are found at about 10 GPa in iodine.[21] This transition is followed by a incommensurable modulated phase[21,22] and by the dissociation of the diatomic molecule at higher pressures.[23] However, the pressure evolution of the polyiodide species will be also affected by the evolution of the confinement volume of the SWCNT under high pressure.

Only few papers dedicated to polyiodide studies under pressure have been published.[11,24] Sengupta *et al.* suggest the breaking of pentaiodide into I_2 and triodide species at low pressure (0.2 GPa) in polymers doped with iodine in aqueous solution. Venkateswaran *et al.* used iodine in a vapor phase to dope SWCNT. No pressure dependence of the I_n^- structural properties is reported. They analyzed their results in terms of different intercalation sites within bundles of SWCNT under pressure.

By contrast, when doping is performed in the liquid phase, recent papers clearly showed that iodine species are located inside the hollow core of SWCNT.[5,6] In the present work, using molten iodine for the doping, we explore the structural transformations of confined polyiodides into SWCNT under pressure. Raman spectroscopy investigations are carried out between 0 and 17 GPa.

II. EXPERIMENTAL

Electric arc discharge commercial MER corporation (http://www.mercorp.com/) highly purified SWCNT were outgassed and annealed at 250 °C for 24 h under dynamical vacuum to remove adsorbed water. Sample characterizations by TEM, x-ray and neutron diffraction reveal a high degree of purity and homogeneity, and a size of bundles around 50 tubes. The diameter distribution is centered at 1.3 nm with a full width of 0.2 nm. A fit of the bare SWCNT diffraction peaks yields a distance between two adjacent nanotubes in a bundle of 17 ± 1 Å. Due to the purification process these tubes have many defects and are opened. Iodine doping of the carbon materials is then achieved by immersing the nanomaterials in molten iodine in evacuated quartz tubes at a temperature of 140 °C for 3 days to perform a saturation doping. The excess iodine is removed by the cold point method and by washing with ethanol afterwards.

Experiments are performed on a Jobin Yvon T 64000 micro-Raman spectrometer. The Raman spectra are recorded with the 514.5 nm excitation wavelength. The laser power used was adjusted to 0.7 mW with a spot diameter of about 3 μm using a 50× objective. Pressure experiments up to 17 GPa are carried out with a diamond-anvil cell using argon as transmitting medium and the ruby fluorescence method for pressure calibration. Four different samples are investigated in separated pressure cell loadings. Since data from the different experiments are comparable, the result of a single representative pressure experiment is presented herein.

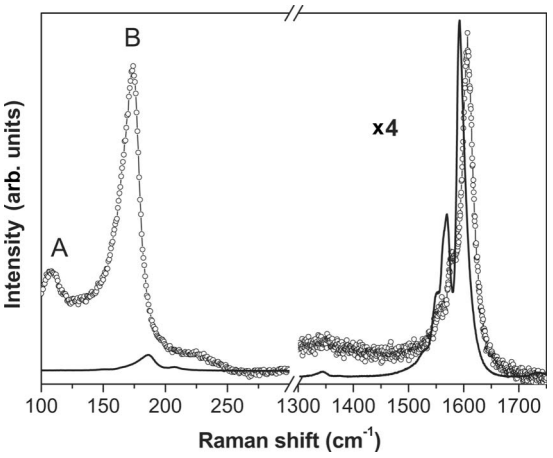

FIG. 1. Normalized Raman spectra recorded at 514.5 nm of raw SWCNT (line) and I@SWCNT (open circles) at room pressure.

III. RESULTS

Figure 1 displays normalized Raman spectra of the raw nanotubes (line) and the iodine intercalated nanotubes (open circles) which exhibit two main regions. The first one is around 1600 cm^{-1} and assigned to the tangential modes (G band) of SWCNT. The G band profile clearly corresponds to semiconducting tubes, as expected at this wavelength (541.5 nm) for such tube diameters (around 1.3 nm). This band upshifts after intercalation of about 15 cm^{-1}. As encapsulation of various noncharged species having different geometries (C_{60}, conjugated oligomers, etc.) inside SWCNT does not alter the G band position, we assign this upshift to a charge transfer between iodine and nanotubes.[7,9]

The second region (between 100 and 250 cm^{-1}) strongly differs between the pristine and the intercalated tubes. In the case of raw tubes, the radial breathing modes (RBMs) are visible with two modes at 187 and 207 cm^{-1}. The iodine intercalated tubes exhibit two broad and prominent bands (labeled A and B), at lower frequencies (109 and 174 cm^{-1}), which can be either the signature of short polyiodide chains[9–18] (Table I) and/or RBM of SWCNT. However the intensity ratio between the low-frequency modes and the G band is not consistent with usual results obtained on pristine nanotubes. In addition, previous Raman measurements on multiwalled nanotubes (without RBM) clearly showed the appearance of both A and B bands after iodine intercalation.[13] Consequently, these modes can be unambiguously assigned to the presence of polyiodides (I_n^{-m} chains).

Raman studies on iodine intercalated organic compounds usually report the presence of only two modes located

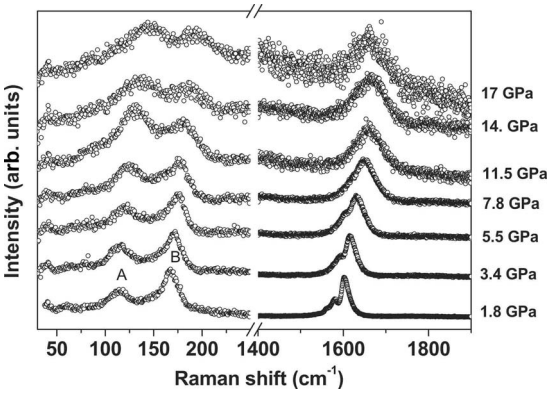

FIG. 2. Selected normalized Raman spectra of I@SWCNT under pressure (from 1.8 to 17 GPa). Two regions can be distinguished: the low-energy one with peaks labeled A and B which correspond to polyiodide modes and the high-energy region with the SWCNT G bands.

around 109 and 174 cm^{-1}, assigned to the vibrations of I_3^- and I_5^- polyiodides, respectively.[9–13] However, the situation is much more complex as we will observe later on by fitting the data (Fig. 3, bottom left). It turns out that seven peaks located at 175, 169, 160, 146, 129, 111, and 104 cm^{-1} are required to fit properly the spectrum, featuring the presence of various polyiodide species in our samples.

Let us now discuss the assignment of the different low-energy modes. The mode at 175 cm^{-1} is usually assigned to the vibration of elongated di-iodine interacting with donors. Solid iodine exhibits a Raman mode at 180 cm^{-1} but, as I_2 becomes coordinated to a donor, the force constant is reduced and the mode moves toward lower wave number (around 175 cm^{-1}).[14–18] From the inspection of Table I, we can assume that the remaining peaks contributing to the "B band" located between 120 and 170 cm^{-1} can be associated to I_n^- species of different geometries (linear, V or L shaped).

In the case of the "A band" the peak around 110 cm^{-1} can arise either from I_3^- (symmetric or asymmetric) or from I_5^- chains (Table I). The classical attribution is the symmetric I_3^- anion with Raman band at 110 cm^{-1} which should be very intense. In our sample, this A band intensity is quite weak with respect to the B band intensity indicating that the presence of symmetric I_3^- anion is very small or negligible. This is in fact, confirmed by EXAFS investigations of I@SWCNT which clearly show no signature of the presence of the expanded I-I distance of the symmetric I_3^- chains.[12] In conclusion, the "A band" can be assigned either to I_5^- anions or asymmetric I_3^- (see Table I). Furthermore, the presence of I_5^- polyiodide can also account for the weak peak observed around 104 cm^{-1}.[14–17] Another possible assignment is lattice librational modes that are observed for iodine single crystal in a frequency range around 110 cm^{-1}.[25,26]

Figure 2 displays Raman profiles of our I@SWCNT as a function of the applied pressure. The left part concerns the low-frequency range where the modes corresponding to the iodine chains are observed. Both bands upshift upon pressure and we can also observe a change in the relative intensity of features A and B between 7.8 and 11.5 GPa. It is worth mentioning that our data are surprisingly very different from those in Ref. 11 (iodine intercalated nanotubes) but similar to those of Ref. 24 (iodine intercalated polyvinyl alcohol). We note that the position of the A and B bands, as well as their pressure evolution, clearly differ from the case of pristine iodine, as an additional proof of the intercalation process.[21] The right part of Fig. 2 displays the tangential G modes of SWCNT. The pressure clearly leads to a strong modification of the G band profiles. The peaks become progressively broader under pressure. In addition, without normalization, a progressive decrease in the associated intensities is exhibited (not shown). The loss in intensity is probably due to a loss of the resonance conditions for SWCNT. A similar behavior is generally observed in empty SWCNT.[27]

Figure 3 exhibits the fits of the iodine (left part) and the SWCNT (right part) modes for some specific values of applied pressure. To follow the peak evolutions, we have to keep in mind that the mode upshift under pressure as evidenced on Fig. 2. The very first pressure effect is to reduce the number of peaks, as observed between 0 and 3.4 GPa. In particular, at 3.4 GPa, the peak at 175 cm^{-1}, assigned to the stretching of I_2 molecules in interaction has disappeared. This change is concomitant with an increase in the intensity of the peak located below 110 cm^{-1}. Increasing the pressure up to 3.4 GPa induces the merging of the two lowest frequencies modes of the A band, giving rise to a single and quite intense peak around 115 cm^{-1}.

Furthermore, some more peaks on the low-frequency side of the B band have disappeared, emphasizing the strong modifications of the polyiodide structural properties. The relative intensity of the main modes (115 and 172 cm^{-1}) has significantly changed with respect to the spectrum at room pressure, meaning that the intensity of the mode located at 115 cm^{-1} increases much more quickly than the peak intensity at 172 cm^{-1}. From 3.4 to 15 GPa, the most important change concerns the relative intensity of the remaining peaks. At 12.2 GPa (not shown), there are only two peaks left and the intensities keep changing drastically. At 15 GPa, the peak located at the lowest frequency is much more intense than the other one. There is no significant change by increasing the pressure up to 17 GPa. Finally, back to the room pressure, only three peaks (176, 166, and 111 cm^{-1}) are observed. The profiles of the Raman spectra are rather different before and after the cycle, meaning that irreversible significant modifications of the polyiodide structural properties take place. Another important point concerns the polyiodide peaks which are much less intense after the pressure cycle with respect to the G band intensity. This indicates dramatic changes in the charged species, leading to a decrease in the charge transfer between the iodine and the nanotubes, in agreement with the G band downshift. For SWCNT, most of the peaks of the G band progressively vanish under pressure. At 15 GPa, only one peak is required to fit properly the data. However, unlike the polyiodide modes, all the peaks (eight) are recovered back to the normal conditions, meaning that the modifications are nearly fully reversible for SWCNT. In fact, there is a difference concerning the peak positions. Indeed, all the peaks are downshifted (between 7 and 11 cm^{-1} depending on the peak) back to the ambient pressure with respect to the very first spectrum before the cycle. In this case, the peak positions are very close

(1596 cm^{-1}) to those measured in the pristine nanotubes (1592 cm^{-1}). This behavior supports a drop in the charge transfer between iodine species and SWCNT after the cycle, consistent with the important decrease in the polyiodide peak intensities.

In Fig. 4 are reported the positions of peaks associated to iodine chains (below 200 cm^{-1}) together with the G band position of I@SWCNT (above 1550 cm^{-1}) under pressure. All the modes reported are derived from the fits displayed on Fig. 3. Both polyiodide and SWCNT modes clearly exhibit at least two regimes. For polyiodide species, a clear transition between two regimes occurs around 2.3 GPa and is evidenced by a merging and/or a disappearance of few modes together with a change in the Raman band pressure dependences. The second transition around 9 ± 1 GPa concerns the SWCNT and leads to significant changes in the Raman mode pressure dependences. At the first sight, the pressure dependence of the polyiodide modes does not look affected by the SWCNT transition. For SWCNT, between ambient pressure and 9 GPa, an important upshift of the SWCNT G band (around 8 ± 2 cm^{-1}/GPa depending on the peak studied) is observed. Beyond 9 GPa, one of the G band peaks disappears and the positions of the two others are rather constant. At 15 GPa, only one peak is observed. This behavior displaying two regimes under pressure has been already observed in raw SWCNT[28] as well as in SWCNT filled with C_{70} fullerenes[29] and in double-well carbon nanotubes.[30] Both experiments and calculations suggest to associate this behavior to a collapse which is defined here as a flattening or a transformation to peanutlike nanotube cross section (see schematic above Fig. 4). The collapse is preceded by the ovalization of carbon nanotubes at lower pressures. Considering the diameter of our tubes, ovalization is typically observed between 1 and 3 GPa and progress continuously up to the collapse pressure. Based on polyiodide Raman mode modifications, we suggest that ovalization takes place around 2.3 GPa and progress up to the collapse transition which takes place at 9 ± 1 GPa. It is noteworthy that this transition around 9 GPa is concomitant with a change in the evolution of the relative intensity of the A and B bands in the low frequency range, assigned to the I_n^{-m} chains fingerprints (Fig. 2). To emphasize this point, the relative intensity of both bands (integrated intensity of band A over integrated intensity of band B, triangles) under pressure is reported on Fig. 5 together with the frequency of the more intense SWCNT G peak (circles). We can notice a clear relationship in both behaviors as a function of the pressure applied. Indeed, the intensity ratio slightly increases during the ovalization process, from ambient pressure to 9 GPa. After the nanotube collapse, there is a significant change in the intensity ratio evolution, meaning that the structural transformations of the polyiodides are favored after the nanotube collapse. Thus, the band positions associated to the iodine species do not look affected by the SWCNT transition according to the pressure dependence of the frequencies. By contrast, the intensity ratio is very sensitive to the SWCNT collapse.

IV. DISCUSSION

We must first mention high-pressure experiments performed on pristine SWCNTs coming from exactly the same sample source.[27,31] Results mainly show that at an excitation wavelength of 541.5 nm with argon as pressure-transmitting medium, no phase transition is observed on the G band position up to 40 GPa.[31] By contrast, other experiments display transition around 11 GPa.[27] In fact, such a transition is not systematically observed and when it is, the transition pressure values vary between 10 and 15 GPa, depending on sample inhomogeneities or differences in the experimental protocols.[27] It has been recently shown that the nanotube homogeneous filling can dramatically stabilize carbon nanotubes toward the collapse pressure while inhomogeneous filling can play the reverse role.[32] In the case of open-ended SWCNT similar to the ones used in our study, the collapse pressure has been observed from 11 GPa in some cases and in others not observed even up to 40 GPa or higher, which probably can be related to the sample's argon filling degree and homogeneity. As mentioned in the experimental section, we performed our experiment on iodine inserted SWCNTs several times and we found out a reproducible behavior, in particular, concerning the correlation between tube and polyiodide responses. However, pressures at which the modifications take place differed from one experiment to another (from 7 to 9 GPa), which probably indicate differences in iodine filling or mixtures or argon/iodine filling.

As previously shown, pressure strongly affects the polyiodide vibrational properties since we can observe the disappearance of many modes between ambient pressure and 3.4 GPa (110, 129, 146, and 175 cm^{-1}) together with an intensity inversion between the bands A and B (Fig. 3). Thus, one of the very first effects of the pressure seems to be the transformation of L- or V-shaped polyiodides into linear chains (Table I), accounting for the disappearance of few modes (129 and 146 cm^{-1}) observed at 2.5 GPa (Fig. 4). Between ambient pressure and 1.8 GPa, a progressive decrease in the peak intensity at 175 cm^{-1} is concomitant with an increase in the peak intensity at 117 cm^{-1}. One possible explanation is the decomposition of I_2 molecules into I_3^- and/or I^- and I^+ ions as proposed by Corban *et al.*[33] At 3.4 GPa, both contributions have vanished, suggesting the decomposition of both I_2 and symmetric I_3^- species.

Further evolutions of the Raman spectra at higher pressure can be interpreted with two possible scenarios detailed below. The first possible scenario to account for our data is the following: at 3.4 GPa, there is only one peak left into the A band at 115 cm^{-1}. According to Table I, this feature corresponds to the symmetric I_3^- species fingerprint (taking into account the pressure induced shift). Since the A over B bands intensity ratio increases, one possible assumption is a transformation of I_5^- polyiodides into I_3^- chains. The modification of the geometry and volume defined by the nanotubes and their progressive ovalization should account for these changes.

Such a scenario has been already used to explain Raman results obtained on polyiodides in poly(vinyl alcohol) films.[24] However, this scenario is not fully satisfactory. Indeed, the symmetric I_3^- chain is expected to have covalent bonding,[17] so that the peak at 110 cm^{-1} should remain intense back to the ambient conditions, unlike our Raman results. In addition, after releasing the pressure, a peak at 175 cm^{-1} is observed, suggesting that I_2 molecules are

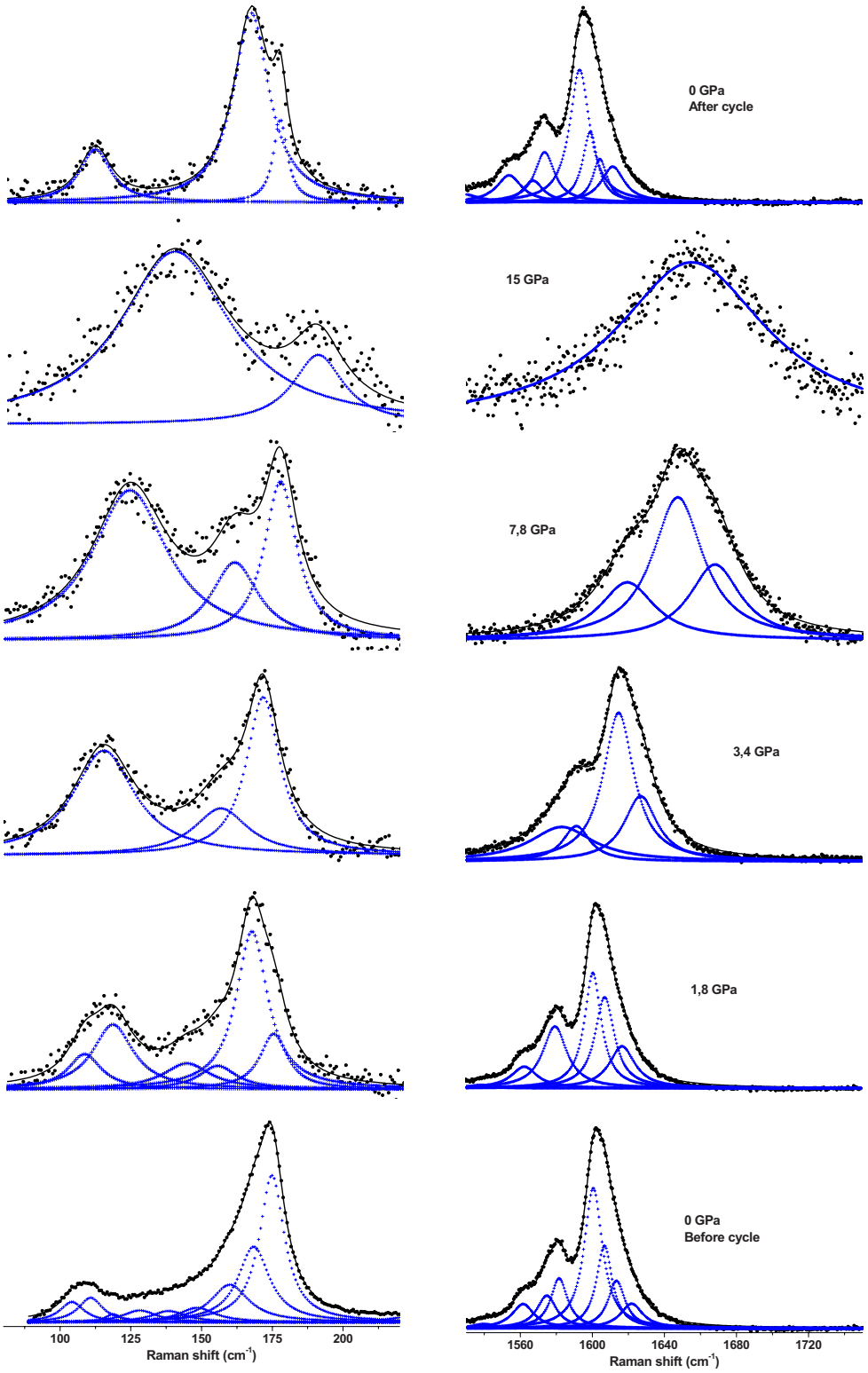

FIG. 3. (Color online) Normalized Raman modes ($\lambda = 514.5$ nm) of polyiodides (left) and SWCNT (right) as a function of the pressure applied (from bottom to top: 0, 1.8, 3.4, 7.8, 15, and 0 GPa after the cycle). Black circles correspond to the experimental data, straight lines correspond to the total fit, and blue crosses are the different peaks used in the fit.

formed again. A similar behavior has been already observed in iodine encapsulated SWCNT under temperature treatment and has been interpreted by structural conversion of polyiodides into molecular iodine.[8] However, since our Raman data show that the peak of the iodine species located at the lowest frequency is a bit more intense and narrower after the pressure treatment (Fig. 3), it is probable that few symmetric I_3^- chains are nevertheless formed under pressure.

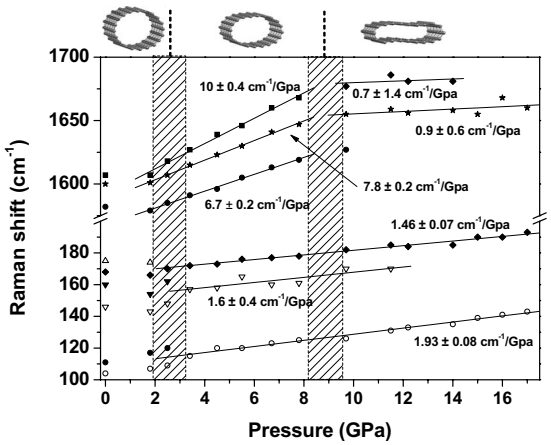

FIG. 4. Main Raman band positions of I@SWCNT under pressure (from 0 to 17 GPa). The hatched regions correspond to transitions between different regimes for polyodides and SWCNTs. The different regimes are fitted by straight lines.

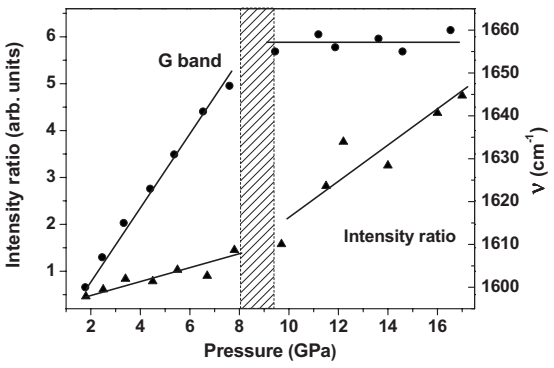

FIG. 5. Relative integrated intensity of B and A bands under pressure (triangles, left scale) together with the G band positions (circles, right scale). The integrated intensities are derived from the peak deconvolution shown in Fig. 3(a). Straight lines are just guides for eyes.

Another possible scenario would consist in considering the A band (around 110 cm^{-1} at ambient pressure) as lattice librational modes as observed in iodine single crystal.[25,26] Within this assumption, the huge increase in the intermolecular mode intensity (A band) with respect to the intramolecular ones (B band) is assigned to the increase in the interaction between polyiodides associated to an electronic rearrangement. As the pressure increases, the intermolecular or interpolyiodide interaction is getting more and more important with respect to the intramolecular ones, leading to a charge delocalization outside the iodine species, giving rise to a huge increase in the intensity ratio between the lattice and the intramolecular modes. This mechanism is described in iodine single crystal as metallization transition under pressure.[25,26] This scenario is consistent with the intensity ratio evolution reported on Fig. 5 and correlated with the transition regime of SWCNT. Thus, the formation of a new iodine structure would be facilitated by the collapse of the tubes. Such a new structure has been already suggested in SWCNT from TEM investigations, even at room pressure, depending on the tube diameter.[5] Back to the ambient pressure, there is no longer intermolecular interaction and the charge is again localized on "isolated" polyiodides accounting for the modifications observed by Raman spectroscopy (Fig. 3).

Finally, if we consider our data after pressure release, a decrease in the amount of polyiodides signal is accompanied by a reduction in the charge amount transferred to the nanotube. This could be explained by a scenario in which the collapsed tube bundle geometry combined with probable argon intrusion inside the tubes could lead to the progressive extraction of iodine from inside the tubes. Under high pressure, the strong nanoconfinement imposed by the collapsed geometry inside and outside the tubes would lead then to the observed tendency to polyiodide linearization. On pressure release, the iodine species found outside the tubes will be able to find a new equilibrium form leading to a reduction in charge transfer to the tubes. In order to go further in our understanding, x-ray absorption near-edge structure and EXAFS investigations under pressure are in progress to get some additional information on both electronic structural properties of iodine species.

V. CONCLUSION

We have investigated the pressure-induced effect on iodine intercalated single-walled carbon nanotubes using Raman spectroscopy. The pressure allows modifying the charge transfer in the hybrid system. Both behaviors of nanotubes and polyiodides are strongly correlated and display several regimes under pressure. Between ambient pressure and 3.4 GPa, an irreversible vanishing of some polyiodide modes is exhibited, indicative of iodine polyanion linearization and decomposition of I_2 molecules. From 3.4 GPa, important reversible changes in the intensity modes are observed. Two scenarios are proposed to account for the modifications under nanoconfinement. The first one assumes the transformation of I_5^- species into I_3^- polyiodides under pressure. The second scenario suggests a progressive metallization process of the polyiodide. This last hypothesis brings new lighting for the understanding of iodine intercalated compounds.

[1] N. A. Kiselev, R. M. Zakalyukin, O. M. Zhigalina, N. Grobert, A. S. Kumskov, Yu. V. Grigoriev, M. V. Chernysheva, A. A. Eliseev, A. V. Krestinin, Yu. D. Tretyakov, B. Freitag, and J. L. Hutchison, J. Microsc. **232**, 335 (2008).

[2] C. G. Xu, J. Sloan, G. Brown, S. Bailey, V. C. Williams, S. Friedrichs, K. S. Coleman, E. Flahaut, J. L. Hutchison, R. E. Dunin-Borkowski, and M. L. H. Green, Chem. Commun. (Cambridge) **2000**, 2427.

[3] A. Ilie, J. S. Bendall, D. Roy, E. Philp, and M. L. Green, J. Phys. Chem. B **110**, 13848 (2006).
[4] G. Pagona, G. Rotas, A. N. Khlobystov, T. W. Chamberlain, K. Porfyrakis, and N. Tagmatarchis, J. Am. Chem. Soc. **130**, 6062 (2008).
[5] L. Guan, K. Suenaga, Z. Shi, Z. Gu, and S. Iijima, Nano Lett. **7**, 1532 (2007).
[6] X. Fan, E. C. Dickey, P. C. Eklund, K. A. Williams, L. Grigorian, R. Buczko, S. T. Pantelides, and S. J. Pennycook, Phys. Rev. Lett. **84**, 4621 (2000).
[7] N. Bendiab, R. Almairac, S. Rols, R. Aznar, J.-L. Sauvajol, and I. Mirebeau, Phys. Rev. B **69**, 195415 (2004).
[8] Z. Y. Wang, L. Wang, Z. J. Shi, J. Lu, Z. N. Gu, and Z. X. Gao, Chem. Commun. (Cambridge) **2008**, 3429.
[9] L. Grigorian, K. A. Williams, S. Fang, G. U. Sumanasekera, A. L. Loper, E. C. Dickey, S. J. Pennycook, and P. C. Eklund, Phys. Rev. Lett. **80**, 5560 (1998).
[10] W. Zhou, S. Xie, L. Sun, D. Tang, Y. Li, Z. Liu, L. Ci, X. Zou, G. Wang, P. Tan, X. Dong, B. Xu, and B. Zhao, Appl. Phys. Lett. **80**, 2553 (2002).
[11] U. D. Venkateswaran, E. A. Brandsen, M. E. Katakowski, A. Harutyunyan, G. Chen, A. L. Loper, and P. C. Eklund, Phys. Rev. B **65**, 054102 (2002).
[12] T. Michel, L. Alvarez, J.-L. Sauvajol, R. Almairac, R. Aznar, J.-L. Bantignies, and O. Mathon, Phys. Rev. B **73**, 195419 (2006).
[13] T. Michel, L. Alvarez, J. L. Sauvajol, R. Almairac, R. Aznar, O. Mathon, J.-L. Bantignies, and E. Flahaut, J. Phys. Chem. Solids **67**, 1190 (2006).
[14] P. Deplano, F. Devillanova, J. Ferraro, M. L. Mercuri, V. Lippolis, and E. Trogu, Appl. Spectrosc. **48**, 1236 (1994).
[15] R. C. Teitelbaum, S. L. Ruby, and T. J. Marks, J. Am. Chem. Soc. **101**, 7568 (1979).
[16] P. Deplano, F. A. Devillanova, J. R. Ferraro, F. Isaia, V. Lippolis, and M. L. Mercuri, Appl. Spectrosc. **46**, 1625 (1992).
[17] P. Deplano, J. Ferraro, M. L. Mercuri, and E. Trogu, Coord. Chem. Rev. **188**, 71 (1999).
[18] P. Svensson and L. Kloo, Chem. Rev. **103**, 1649 (2003).
[19] S. Hsu, A. Signorelli, G. Pez, and R. Baughman, J. Chem. Phys. **69**, 106 (1978).
[20] A. San-Miguel, H. Libotte, M. Gauthier, G. Aquilanti, S. Pascarelli, and J.-P. Gaspard, Phys. Rev. Lett. **99**, 015501 (2007).
[21] T. Kume, T. Hiraoka, Y. Ohya, S. Sasaki, and H. Shimizu, Phys. Rev. Lett. **94**, 065506 (2005).
[22] T. Kenichi, S. Kyoko, F. Hiroshi, and O. Mitsuko, Nature (London) **423**, 971 (2003).
[23] Y. Fujii, K. Hase, Y. Ohishi, H. Fujihisa, N. Hamaya, K. Takemura, O. Shimomura, T. Kikegawa, Y. Amemiya, and T. Matsushita, Phys. Rev. Lett. **63**, 536 (1989).
[24] A. Sengupta, E. L. Quitevis, and M. W. Holtz, J. Phys. Chem. B **101**, 11092 (1997).
[25] H. Olijnyk, W. Li, and A. Wokaun, Phys. Rev. B **50**, 712 (1994).
[26] A. Congeduti, P. Postorino, M. Nardone, and U. Buontempo, Phys. Rev. B **65**, 014302 (2001).
[27] A. Merlen, P. Toulemonde, N. Bendiab, A. Aouizerat, J. L. Sauvajol, G. Montagnac, H. Cardon, P. Petit, and A. San Miguel, Phys. Status Solidi B **243**, 690 (2006).
[28] M. Yao, Z. Wang, B. Liu, Y. Zou, S. Yu, W. Lin, Y. Hou, S. Pan, M. Jin, B. Zou, T. Cui, G. Zou, and B. Sundqvist, Phys. Rev. B **78**, 205411 (2008).
[29] Ch. Caillier, D. Machon, A. San-Miguel, R. Arenal, G. Montagnac, H. Cardon, M. Kalbac, M. Zukalova, and L. Kavan, Phys. Rev. B **77**, 125418 (2008).
[30] A. L. Aguiar *et al.* (unpublished).
[31] A. Merlen, N. Bendiab, P. Toulemonde, A. Aouizerat, A. San Miguel, J. L. Sauvajol, G. Montagnac, H. Cardon, and P. Petit, Phys. Rev. B **72**, 035409 (2005).
[32] A. San Miguel, C. Caillier, D. Machon, E. B. Barros, A. L. Aguiar, and A. G. Souza Filho, *Crystallography at High Pressure*, NATO Science for Peace and Security Series B: Physics and Biophysics (Springer, Dordrecht, 2010), pp. 435–446.
[33] G. J. Corban, C. Antoniadis, S. K. Hadjikakou, N. Hadjiliadis, J. F. Meng, and I. S. Butler, Bioinorganic Chem. Applications **1**, 68542 (2006).